

# Si<sub>3</sub>N<sub>4</sub>/CrN nanostructured multilayers grown by RF reactive magnetron sputtering<sup>①</sup>

JIANG Shihang(姜世杭)<sup>1</sup>, XU Jun-hua(许俊华)<sup>2</sup>, LI Ge-yang(李戈扬)<sup>2</sup>

(1. Department of Mechanical Engineering, Yangzhou University, Yangzhou 225009, China;  
2. State Key Lab of Metal Matrix Composites, Shanghai Jiaotong University, Shanghai 200030, China)

**Abstract:** The amorphous/ polycrystalline Si<sub>3</sub>N<sub>4</sub>/CrN nanostructured multilayer films have been prepared by radio frequency (RF) reactive magnetron sputtering. The composition, microstructure and mechanical properties of these films were characterized by X-ray photoelectron spectroscopy (XPS), X-ray diffraction (XRD), high-resolution transmission electron microscopy (HRTEM) and nanoindentation. The CrN and Si<sub>3</sub>N<sub>4</sub> single layer films are polycrystalline face centered cubic and amorphous structures, respectively. The CrN and Si<sub>3</sub>N<sub>4</sub> layers are nearly stoichiometric. The HRTEM image indicates that the interfaces are planar and modulation structure is clear in multilayers. The hardness values of Si<sub>3</sub>N<sub>4</sub>/CrN multilayers are between those of the constituent CrN and Si<sub>3</sub>N<sub>4</sub> films at a substrate temperature of 20 °C, and are somewhat higher than those of Si<sub>3</sub>N<sub>4</sub> films at a deposition temperature of 500 °C. There is no superhardness effect in the Si<sub>3</sub>N<sub>4</sub>/CrN multilayers. Based on the experimental results, the hardening mechanisms in the multilayers have been discussed.

**Key words:** physical vapor deposition; Si<sub>3</sub>N<sub>4</sub>/CrN; multilayers; microstructure; mechanical properties

**CLC number:** O 484

**Document code:** A

## 1 INTRODUCTION

In recent years, ceramic superhardness compositionally-modulated multilayer films have been actively investigated<sup>[1-8]</sup>. The research results show that multilayers can combine the properties of the constituent materials and have more excellent properties than those of the single-layer film. A large number of internal interfaces which are parallel to the substrate surface can retard crack propagation and provide barriers to dislocation movement. Multilayers with optimized interface areas seem to be most promising with respect to an optimum hardness-to-toughness ratio<sup>[9-12]</sup>.

TiN films deposited by physical vapor deposition (PVD) or chemical vapor deposition (CVD) have found widespread applications in wear resistant situations such as cutting tools or machine parts because of their high hardness, chemical inertness and high temperature stability. However an increasing attention is focused on other metal nitrides grown by PVD processes beside the investigation of TiN-based films, during recent years, such as CrN and Si<sub>3</sub>N<sub>4</sub><sup>[13-16]</sup>. Because of the excellent mechanical and tribological properties for specific applications of CrN and Si<sub>3</sub>N<sub>4</sub> single-layer films, a new kind of Si<sub>3</sub>N<sub>4</sub>/CrN nano-multilayers has been prepared by reactive magnetron sputtering process. In this paper, the effects of modulation periods, modulation ratio and deposition temperature on microhardness have been investigated.

## 2 EXPERIMENTAL

CrN and Si<sub>3</sub>N<sub>4</sub> single-layer films and Si<sub>3</sub>N<sub>4</sub>/CrN multilayer films with different modulation periods were prepared using a radio frequency (RF) magnetron sputtering setup. The sputtering targets were 3-inch single crystal silicon (99.999 999 9%) and pure metal Cr (99.99%). The boron-doped Si(100) wafers used as substrates were first ultrasonically cleaned in acetone, then dipped in a 2% HF solution for 1 min and pure water for 10 min. After drying with dried gas, the sample was mounted on the sample holder and transferred to the sputtering chamber. The sputtering chamber was then evacuated to the routinely achieved base pressure of  $5.0 \times 10^{-8}$  Pa. High-purity argon and nitrogen gases were introduced into the chamber from mass flow controllers. The working pressure was  $2.1 \times 10^{-1}$  Pa with argon and nitrogen gas flows of 4 sccm and 2 sccm. Multilayers were deposited by alternately opening the Si and Cr target shutters, in order to expose the substrate to the plasma from the Cr or Si target. The layer thickness was controlled by both the opening time of the shutters and the target power levels. During deposition, the substrate was rotated to achieve uniform film thickness. The target power was 100 W for Cr and 220 W for Si, and both the deposition rate of CrN and Si<sub>3</sub>N<sub>4</sub> were about 0.80 nm/min. The substrate was heated to a temperature, which was according to the design parameters. The nominal total thickness of the single layer-films and multilayers was 0.3 μm.

to  $1.0 \mu\text{m}$ , respectively.

The X-ray photoelectron spectroscopy (XPS) measurement was carried out by an ESCALAB 220iXL (VG Scientific) type spectrometer, and the monochromatic X-ray source ( $\text{Al K}\alpha$ ) was used. The crystal structure of the single-layer films and multilayer films was determined with a RAD-C X-ray diffractometer using  $\text{Cu K}\alpha$  radiation, operated at 40 kV and 35 mA. The glancing incidence angle was  $1^\circ$  and the scanning speed was  $0.5^\circ/\text{min}$ . The microstructures of these multilayers were characterized by cross-section high-resolution transmission electron microscopy (HRTEM) using a JEM-3000F operation at an accelerating voltage of 300 kV. The hardness of multilayer films was measured by using ENT-1100a nanoindentation hardness tester.

### 3 RESULTS AND DISCUSSION

#### 3.1 XPS and XRD analysis

Fig. 1 and Fig. 2 show the XPS spectra of N 1s and Cr 2p of CrN films and N 1s and Si 2p of  $\text{Si}_3\text{N}_4$  films, respectively. Argon beam sputtering was

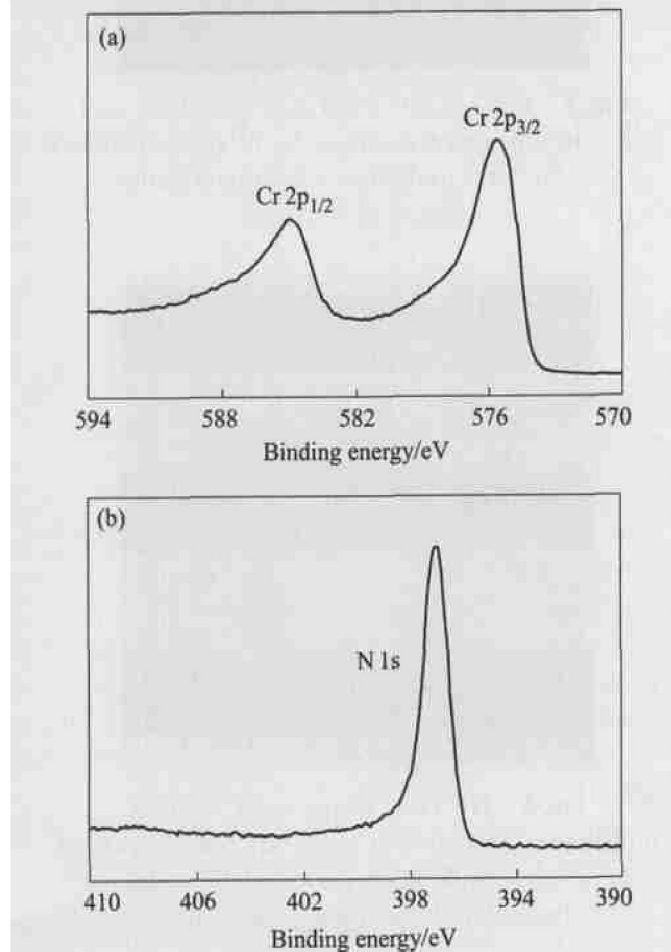


Fig. 1 Cr 2p(a) and N 1s(b) XPS spectra of CrN films

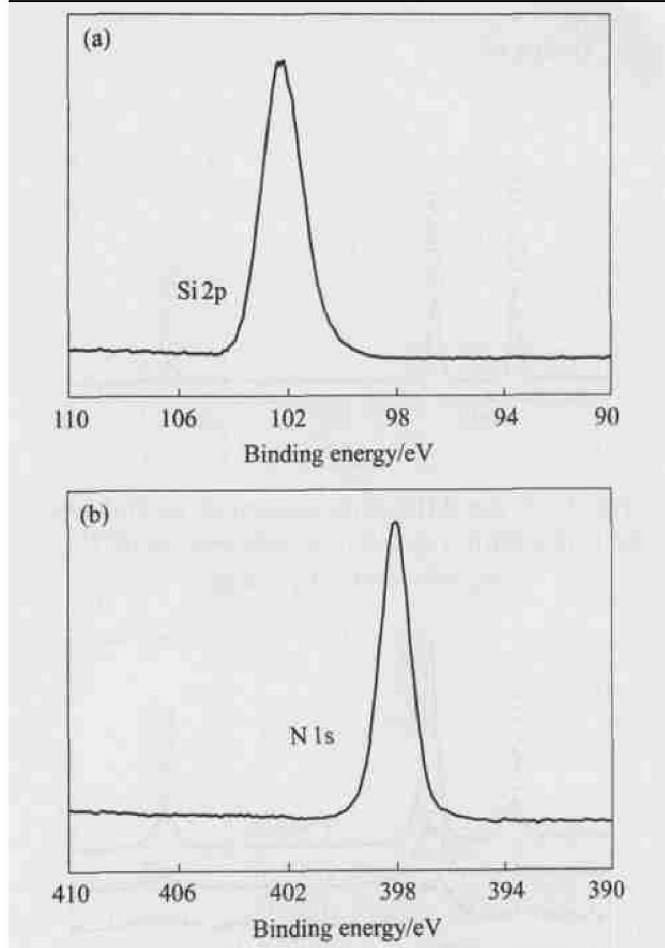
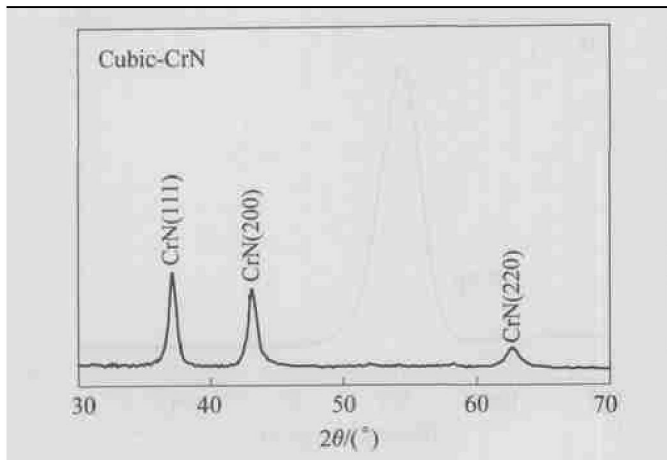


Fig. 2 Si 2p(a) and N 1s(b) XPS spectra of  $\text{Si}_3\text{N}_4$  films

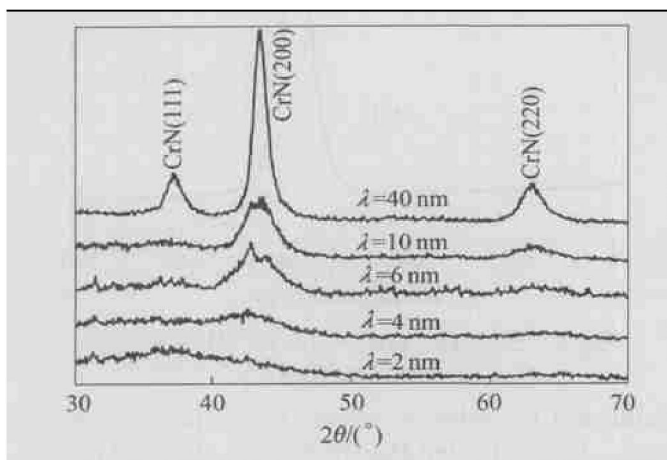
conducted in order to clean the surface of specimens. It is indicated that there is no detectable free nitrogen ( $\text{N}_2$ ), pure Si and metal Cr present in the films. This means that the films are only composed of  $\text{Si}_3\text{N}_4$  or CrN phases. The mean atomic ratio  $n_{\text{N}}/n_{\text{Cr}}$  of CrN films and  $n_{\text{N}}/n_{\text{Si}}$  of  $\text{Si}_3\text{N}_4$  films, determined from corresponding N 1s and Cr 2p or Si 2p core-level intensities after the surface layer contamination is removed by sputtering, are approximately 0.83 and 1.3, which are close to the values of stoichiometric CrN and  $\text{Si}_3\text{N}_4$  films.

Fig. 3 shows the X-ray diffraction spectra of single layer CrN films with  $\text{N}_2$  and Ar gas flows of 2 sccm and 4 sccm, respectively. The CrN (B1 NaCl structure) phase is observed and the lattice constant is 0.4192 nm. The XRD spectra of  $\text{Si}_3\text{N}_4$  single layer films reveal amorphous  $\text{Si}_3\text{N}_4$  films. The XRD spectra of  $\text{Si}_3\text{N}_4/\text{CrN}$  multilayers (Fig. 4) with different modulation periods show that the crystal growth of CrN is interrupted by amorphous  $\text{Si}_3\text{N}_4$  films at smaller modulation periods, leading to the nanocrystalline CrN films (it can be found in Fig. 5 and Fig. 6). With

increasing modulation period, the intensity of main peaks of CrN increases and the full-width at half-maximum decreases. This



**Fig. 3** X-ray diffraction pattern of single layer CrN films with a deposition temperature of 20 °C,  $p_{\text{Ar}} = 4 \text{ sccm}$ ,  $p_{\text{N}_2} = 2 \text{ sccm}$



**Fig. 4** XRD patterns of Si<sub>3</sub>N<sub>4</sub>/CrN multilayers at different modulation periods

means that the grain size of CrN in the multilayers increases with the increase of CrN layer thickness. The face-centered cubic CrN phase with texture (200) can be observed at larger modulation periods.

### 3.2 TEM analysis

The bright-field TEM micrograph and electron diffraction patterns of cross-sectional Si<sub>3</sub>N<sub>4</sub>/CrN multilayers with a modulation period of 40.0 nm are shown in Fig. 5. The TEM image indicates that the interfaces are planar and modulation structure is clear in multilayers. The CrN layers appear darker and Si<sub>3</sub>N<sub>4</sub> layers are brighter because of their different average atomic numbers. The modulation ratio measured from the image is about  $l_{\text{Si}_3\text{N}_4}/l_{\text{CrN}} = 1:1$ . Indexing of Fig. 5(b) shows the multilayers are of face-centered cubic (fcc) crystal structure.

Fig. 6 gives a high-resolution transmission electron microscopy photograph of Si<sub>3</sub>N<sub>4</sub>/CrN multilayers with a modulation period of 10.0 nm. It shows that the CrN layers are nanopolycrystalline and the Si<sub>3</sub>N<sub>4</sub> layers are amorphous.

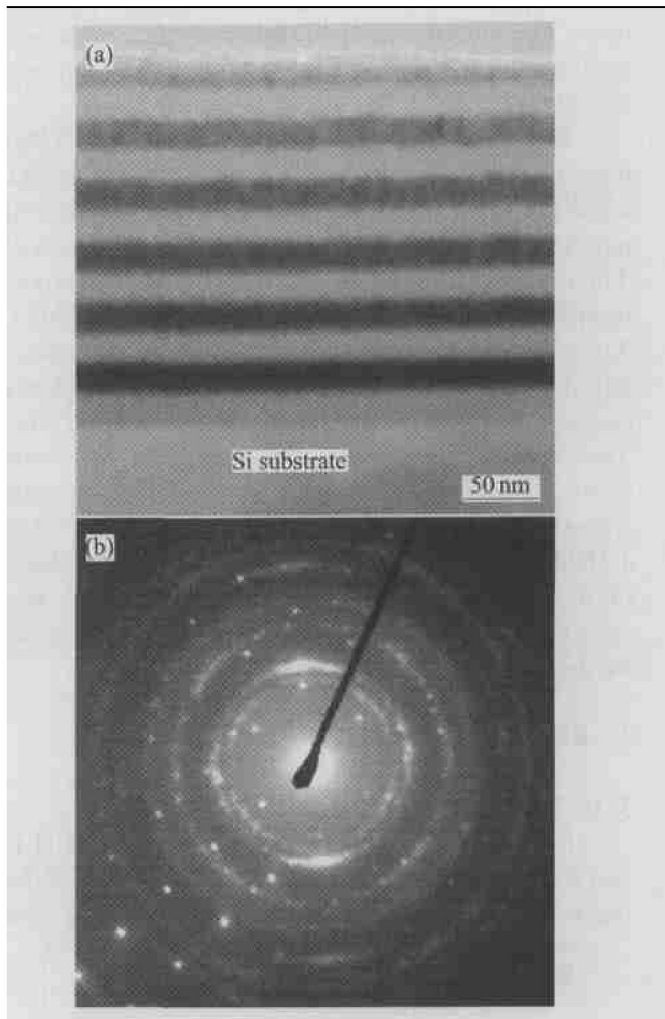


**Fig. 5** Bright-field TEM micrograph(a) and electron diffraction patterns(b) of cross-sectional Si<sub>3</sub>N<sub>4</sub>/CrN multilayers with modulation period of 40.0 nm

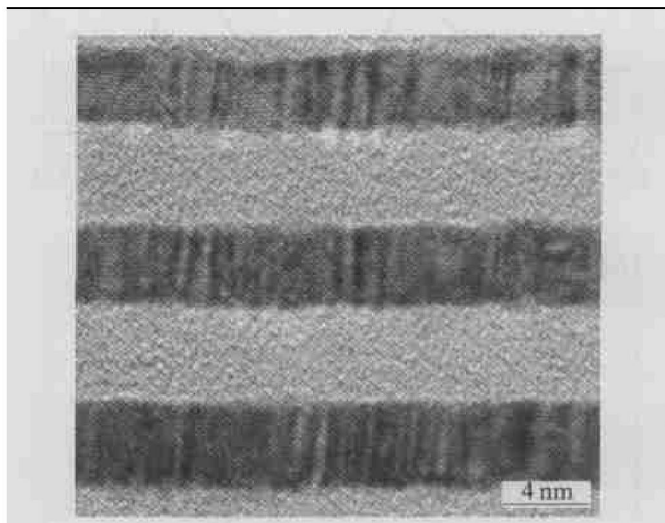


**Fig. 6** HRTEM image of Si<sub>3</sub>N<sub>4</sub>/CrN multilayers deposited at substrate temperature of 20 °C with modulation period of 10.0 nm and modulation ratio ( $l_{\text{Si}_3\text{N}_4}/l_{\text{CrN}}$ ) of 1

### 3.3 Microhardness of films

Fig. 7 shows the hardness of Si<sub>3</sub>N<sub>4</sub>/CrN multi-

layers as a function of the modulation period. The hardness values of the  $\text{Si}_3\text{N}_4/\text{CrN}$  multilayers are between those of constituent monolithic  $\text{CrN}$  and  $\text{Si}_3\text{N}_4$  films with deposition temperature of 20 °C. The hardness values of the multilayers are somewhat higher than those calculated from the rule of mixture, but never reach that of the  $\text{Si}_3\text{N}_4$  monolithic films. However, the hardness values of the  $\text{Si}_3\text{N}_4/\text{CrN}$  multilayers with modulation ratio ( $l_{\text{Si}_3\text{N}_4}/l_{\text{CrN}}$ ) of 1:1 and 3:1 deposited at 500 °C are slightly higher than those of monolithic  $\text{Si}_3\text{N}_4$  films. The modulation ratio does not affect the hardness. The superhardness effect is not present in this system.

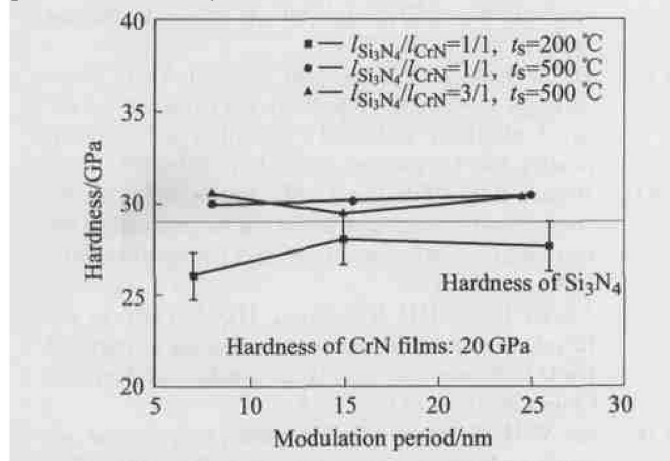


**Fig. 7** Hardness of  $\text{Si}_3\text{N}_4/\text{CrN}$  multilayers as function of modulation period with different modulation ratios and deposition temperatures

According to the Koehler theory<sup>[17]</sup>, the hardness anomalies are due to the modulus difference between the superlattice layers. The hardness enhancement in the multilayers can be calculated through the following equation<sup>[6]</sup>:

$$H = 10 \tau_{\max} = \frac{5RG_{\text{CrN}} \sin \theta}{4\pi} \quad (1)$$

where  $R = (G_A - G_B)/(G_A + G_B)$ .  $G_A$  and  $G_B$  are the shear modulus of materials A and B, respectively. However our experimental results show that the difference of elastic modulus between the constituent materials of  $\text{CrN}$  and  $\text{Si}_3\text{N}_4$  are small. The elastic modulus values of  $\text{CrN}$  and  $\text{Si}_3\text{N}_4$  single layer films are 243.0 and 240.0 GPa. This means that the increase of hardness caused by the Koehler model is slight even if we assume that  $\text{Si}_3\text{N}_4$  layers are polycrystalline in the same way as the  $\text{CrN}$  layers in  $\text{CrN}/\text{Si}_3\text{N}_4$  multilayers.

Another hardening mechanism is the coherency strain effect<sup>[18]</sup>. However, there is no coherent stress between  $\text{CrN}$  and  $\text{Si}_3\text{N}_4$  layers in the multilayers because of the crystal/amorphous interfaces.

Xu et al<sup>[7]</sup> have suggested a hardening mechanism in  $\alpha\text{-Si}_3\text{N}_4/\text{nc-TiN}$  multilayers: heated induced alternating stress fields strengthening. According to

the coherency strain effect<sup>[18]</sup>, the enhancement of strength and hardness of the films is caused by the coherent alternating strain fields. The alternating strain fields, hence stress fields, are caused by the mismatch of thermal expansion coefficients in A/B multilayers. The heated induced alternating stresses are deduced as follows<sup>[7]</sup>:

$$\sigma_{xx}^1 = \sigma_{yy}^1 = \frac{E_1 E_2 d_2 (\alpha_2 - \alpha_1) \Delta T}{(1 - \nu_1) E_2 d_2 + (1 - \nu_2) E_1 d_1} \quad (2)$$

and

$$\sigma_{xx}^2 = \sigma_{yy}^2 = \frac{E_1 E_2 d_1 (\alpha_2 - \alpha_1) \Delta T}{(1 - \nu_1) E_2 d_2 + (1 - \nu_2) E_1 d_1} \quad (3)$$

where  $\sigma_{xx}^1$ ,  $\sigma_{xx}^2$  are the residual compression stresses and residual tensile stresses in layers A and B, respectively.  $E_1$  and  $E_2$ ,  $d_1$  and  $d_2$ ,  $\alpha_1$  and  $\alpha_2$ , and  $\nu_1$  and  $\nu_2$  are elastic modulus, thickness, thermal expansion coefficients, and Poisson's ratios of layers A and B, respectively.  $\Delta T$  is the difference temperature between the room temperature and the deposition temperature. The magnitude of these stresses depends on the mismatch of the thermal expansion coefficient, temperature difference and the relative thickness of the layers.

It is suggested that superhardness effect will appear when there exist alternate stress fields, regardless of the coherency strain or thermal mismatch strain<sup>[7]</sup>. However, the thermal expansion coefficients of  $\text{CrN}$  and  $\text{Si}_3\text{N}_4$  are 2.3 and  $2.5 \times 10^{-6} \text{ K}^{-1}$ , respectively. The difference of thermal expansion mismatch is too close to cause thermal stresses in the  $\text{CrN}$  and  $\text{Si}_3\text{N}_4$  interfaces when we calculate the alternate stresses by Eqns. (2) and (3). In this case, there are not any kinds of alternating stress fields in the films. Hence, no enhancement of hardness contributed by Cahn's coherent stress model occurs. That is the reason why the hardness values of the  $\text{Si}_3\text{N}_4/\text{CrN}$  multilayers deposited at room temperature are between those of the constituent materials. The slight increase of hardness values of the  $\text{Si}_3\text{N}_4/\text{CrN}$  multilayers deposited at 500 °C may contribute to a little increase of alternating stress fields in the multilayers.

#### 4 CONCLUSIONS

A new kind of  $\text{Si}_3\text{N}_4/\text{CrN}$  nano multilayers on Si (100) substrates has been prepared by reactive magnetron sputtering process. The  $\text{CrN}$  and  $\text{Si}_3\text{N}_4$  layers are nearly stoichiometric. The  $\text{CrN}$  and  $\text{Si}_3\text{N}_4$  single layer films are polycrystalline face centered cubic and amorphous structures, and the interfaces are planar and modulation structure is clear in multilayers. The crystal growth of  $\text{CrN}$  is interrupted by amorphous  $\text{Si}_3\text{N}_4$  films at smaller modulation periods, leading to the nanocrystalline  $\text{CrN}$  films. The hardness values of  $\text{Si}_3\text{N}_4/\text{CrN}$  multilayers are between those of the con-

stituent CrN and  $\text{Si}_3\text{N}_4$  films at the substrate temperature of 20 °C, and are somewhat higher than those of  $\text{Si}_3\text{N}_4$  films at the deposition temperature of 500 °C. There is no superhardness effect in the  $\text{Si}_3\text{N}_4/\text{CrN}$  multilayers.

## REFERENCES

[ 1 ] Helmersson U, Todorova S, Barnett S A, et al. Growth of single crystal TiN/ VN strained-layer superlattices with extremely high mechanical hardness[ J]. Journal of Applied Physics, 1987, 62(2): 481 - 484 .

[ 2 ] Mirkarimi P B, Hultman L, Barnett S A. Enhanced hardness in lattice matched single crystal TiN/  $\text{V}_{0.6}\text{Nb}_{0.4}\text{N}$  superlattices[ J]. Applied Physics Letters, 1990, 57( 25): 2654 - 2656.

[ 3 ] Chu X, Barnett S A. Model of superlattice yield stress and hardness enhancements [ J]. Journal of Applied Physics, 1995, 77(9): 4403 - 4411.

[ 4 ] XU Jun hua, GU Ming yuan, LI Ge yang, et al. Microstructures and properties of  $\text{Si}_3\text{N}_4/\text{TiN}$  ceramic nano multilayer films[ J]. Trans Nonferrous Met Soc China, 1999, 9(4): 764 - 767.

[ 5 ] XU Jun hua, LI Ge yang, GU Ming yuan. The microstructure and superhardness effect of the polycrystalline TaN/TiN and TaWN/TiN superlattice flms[ J]. Acta Metallurgica Sinica, 1999, 35(11): 1214 - 1218.

[ 6 ] Xu J, Kamiko M, Zhou Y, et al. Superhardness effects of heterostructure NbN/TaN nanostructured multilayers [ J]. Journal of Applied Physics, 2001, 89(7): 3674 - 3678.

[ 7 ] XU Jun hua, YU Li hua, Kojima I, et al. Thermal stress hardening of  $\alpha\text{Si}_3\text{N}_4/\text{ncTiN}$  nanostructured multilayers[ J]. Applied Physics Letters, 2002, 81(22): 4139 - 4141.

[ 8 ] Li G, Han Z, Tian J, et al. Alternating stress field and superhardness effect in TiN/ NbN superlattice films[ J]. J of Va Sci Technol, 2002, A20(3): 674 - 677.

[ 9 ] Holleck H, Lahres M, Woll P. Multilayer coatings influence of fabrication parameters on constitution and properties[ J]. Surface and Coating Technology, 1990, 41: 179 - 190.

[ 10 ] Bull S J, Jones A M. Multilayer coatings for improved performance [ J]. Surface and Coating Technology, 1996, 78: 173 - 184.

[ 11 ] Huang R F, Wen L S. Microstructural and indentation characterization of Ti/TiN multilayer films[ J]. Surface and Coating Technology, 1992, 50: 97 - 101.

[ 12 ] YU Xiaojiang, LAI Qianxi, LI Ge yang, et al. Mechanical properties and wear resistance of TaN/NbN nano multilayers[ J]. Journal of Materials Science Letters, 2002, 21: 1671.

[ 13 ] Tu Ju Neng, Duh Jenq Gong, Tsai Shu Yueh. Morphology, mechanical properties, and oxidation behavior of reactively sputtered Cr-N films[ J]. Surface Coating and Technology, 2000, 133: 181 - 185.

[ 14 ] Aouadi S M, Schultze D M, Rohde S L, et al. Growth and characterization of  $\text{Cr}_2\text{N}/\text{CrN}$  multilayer coatings [ J]. Surface and Coating Technology, 2001, 140(3): 269 - 277.

[ 15 ] TANG Bin, ZHU Xiaodong, HU Naisai, et al. Effects of intermixing process on bonding strength of IBED CrN coatings[ J]. Trans Nonferrous Met Soc China, 2000, 10(1): 64 - 68.

[ 16 ] Soe W H, Yamamoto R. Mechanical properties of ceramic multilayers: TiN/ CrN, TiN/ ZrN, and TiN/ TaN [ J]. Materials Chemistry and Physics, 1997, 50: 176 - 181.

[ 17 ] Koehler J S. Attempt to design a strong solid[ J]. Physical Review B, 1970, 2: 547 - 551.

[ 18 ] Cahn J W. Hardening by spinodal decomposition[ J]. Acta Metall, 1963, 11: 1275 - 1282.

(Edited by PENG Chao qun)